Radiology

Effect of Resting-State Functional MR Imaging Duration on Stability of Graph Theory Metrics of Brain Network Connectivity[1]

Christopher T. Whitlow, MD, PhD
Ramon Casanova, PhD
Joseph A. Maldjian, MD

Purpose: To investigate the effect of resting-state (RS) functional magnetic resonance (MR) imaging blood oxygen level–dependent (BOLD) signal acquisition duration on stability of computed graph theory metrics of brain network connectivity.

Materials and Methods: An institutional ethics committee approved this study, and informed consent was obtained. BOLD signal (7.5 minutes worth) was obtained from 30 subjects and truncated into 30-second time bins that ranged from 1.5 to 7.5 minutes. A binarized adjacency matrix for each subject and acquisition duration was generated at network costs between 0.1 and 0.5, where network cost is defined as the ratio of the number of edges (connections) in a network to the maximum possible number of edges. Measures of correlation coefficient stability associated with functional connectivity matrices (correlation coefficient standard deviation [SD] and correlation threshold) and associated graph theory metrics (small worldness, local efficiency, and global efficiency) were computed for each subject at each BOLD signal acquisition duration. Computations were implemented with a 15-node 30-core computer cluster to enable analysis of the approximately 2000 resulting brain networks. Analysis of variance and posthoc analyses were conducted to identify differences between time bins for each measure.

Results: Small worldness, local efficiency, and global efficiency stabilized after 2 minutes of BOLD signal acquisition, whereas correlation coefficient data from functional connectivity matrices (correlation coefficient SD and cost-associated threshold) stabilized after 5 minutes of BOLD signal acquisition.

Conclusion: Graph theory metrics of brain network connectivity (small worldness, local efficiency, and global efficiency) may be accurately computed from as little as 1.5–2.0 minutes of RS functional MR imaging BOLD signal. As such, implementation of these methods in the context of time-constrained clinical imaging protocols may be feasible and cost-effective.

Supplemental material: *http://radiology.rsna.org/lookup/suppl/doi:10.1148/radiol.11101708/-/DC1*

[1] From the Advanced NeuroScience Imaging Research Laboratory, Division of Radiologic Sciences, Department of Radiology (C.T.W., J.A.M.), and Division of Public Health Sciences, Department of Biostatistical Sciences (R.C.), Wake Forest University School of Medicine, Medical Center Blvd, Winston-Salem, NC 27157-1088. Received September 17, 2010; revision requested November 8; revision received December 19; accepted December 29; final version accepted January 10, 2011. C.T.W. supported by a Neuroradiology Education & Research Foundation Fellowship Grant from the American Society of Neuroradiology. **Address correspondence to** C.T.W. (e-mail: *cwhitlow@wfubmc.edu*).

Mathematical models for computational network analysis based on graph theory have risen to the forefront of the investigation of brain connectivity as a complex distributed system. Graph theoretical analysis yields a mathematical description of a network that is composed of numerous nodes (vertices) related to one another by edges (connections). Thus, patterns of connectivity within the brain can be modeled as a network of nodes representing brain regions or voxels, with edges representing interregional or intervoxel connections. Networks characterized by many short-distance neighboring connections and a few long-distance connections were first described by Watts and Strogatz (1) and called small-world networks based on the similar properties of complex social networks in which two people selected at random from a large population are connected by a remarkably short chain of intermediate acquaintances (2). Just as the double helix has been found to underlie the organizational architecture of genetic structure across species, small-world network topologies are being shown to underlie the organizational architecture of all manner of complex biologic systems, including the fundamental structural and functional architecture of brain connectivity. The reason brain connectivity may have evolved such network properties could lie in various strategic advantages that are biologically relevant. Others have suggested that small-world topography produces optimal organization for rapid synchronization and information transfer between brain regions (3–7). Small-world networks demonstrate high local and global efficiency, requiring minimal wiring costs and resulting in balance between local processing and global integration (3,4,8,9).

Graph theory network analyses applied to blood oxygen level–dependent (BOLD) data extracted from resting-state (RS) functional magnetic resonance (MR) images have begun to shed light on changes in the central nervous system at the level of whole-brain distributed network connectivity that appear to underlie a variety of neurodegenerative and psychiatric disorders, such as Alzheimer disease, schizophrenia, attention deficit hyperactivity disorder, and multiple sclerosis (10–17). The ability to identify disease-associated changes in brain connectivity is important, as such changes may represent functional markers of disease that could facilitate better diagnosis and prediction of central nervous system dysfunction in the future.

Several steps are generally necessary to construct functional brain networks and compute graph theory metrics. These include collecting RS functional MR imaging BOLD time course data from nodes or defined anatomic units (regions of interest or voxels), estimating a correlation coefficient matrix between all nodes to define network edges or functional connections, and thresholding the correlation matrix (Cij) to generate a binary association or adjacency matrix from which graph theory metrics are computed (18,19). RS functional MR imaging BOLD data are collected with a variety of acquisition durations, but the general duration is 5–15 minutes (20,21). The length of time required to collect BOLD data can be problematic within a constrained clinical MR imaging time slot, particularly when an imaging protocol includes additional relatively long MR sequences, such as diffusion-tensor imaging, perfusion imaging, or task-based functional MR imaging. Long MR sequences can also be problematic in populations that are challenging to examine, such as young children and critically ill patients. Recent work by Van Dijk and colleagues (22) has suggested that for BOLD data acquisition a duration of approximately 5 minutes is necessary for stabilization of average correlation strengths associated

Advances in Knowledge

- As little as 2 minutes of resting-state functional MR imaging blood oxygen level dependent (BOLD) signal is sufficient to accurately compute frequently used graph theory metrics of brain network connectivity; this short duration suffices even though longer acquisition durations are required for stabilization of the functional MR imaging time series correlations from which the graph theory metrics are computed.
- Stabilization of graph theory metrics occurs along different temporal trajectories than that for connectivity correlation matrices.

Implications for Patient Care

- The relatively short BOLD signal acquisition durations required to accurately compute graph theory metrics make clinical implementation of network connectivity graph theoretical analyses feasible and cost-effective, even in populations that pose challenges to the time constraints of routine imaging, such as young children and critically ill patients.
- The clinical implementation of network connectivity graph theoretical analyses is important, as such data may yield functional markers of disease that improve the ability to diagnose and predict outcomes associated with central nervous system dysfunction in the future.

Published online before print
10.1148/radiol.11101708

Radiology 2011; 259:516–524

Abbreviations:
ANOVA = analysis of variance
BOLD = blood oxygen level–dependent
CI = confidence interval
Cij = correlation matrix
RS = resting state
SD = standard deviation

Author contributions:
Guarantors of integrity of entire study, C.T.W., J.A.M.; study concepts/study design or data acquisition or data analysis/interpretation, all authors; manuscript drafting or manuscript revision for important intellectual content, all authors; manuscript final version approval, all authors; literature research, all authors; experimental studies, all authors; statistical analysis, all authors; and manuscript editing, all authors

Potential conflicts of interest are listed at the end of this article.

See also the editorial by Petrella in this issue.

with the RS functional MR time series data. However, little is known about the RS functional MR imaging BOLD data collection duration required to generate stable and reliable graph theory network metrics of brain network connectivity, which would be important information for practical clinical implementation of these methods.

In the present study, functional brain network connectivity graph theoretical analyses were applied to a series of incrementally longer temporal epochs of RS functional MR imaging data acquired from healthy volunteers. We hypothesized that correlations between regions of interest in RS functional MR imaging data and the corresponding graph theory metrics may stabilize along different temporal trajectories, requiring different durations of RS functional MR imaging BOLD signal acquisition for optimal characterization. Such data are important for establishing efficient and cost-effective MR imaging protocols necessary to implement network connectivity graph theoretical analyses in clinical practice. The purpose of this study was to investigate the effect of RS functional MR imaging BOLD signal acquisition duration on the stability of computed graph theory metrics of brain network connectivity.

Materials and Methods

Participants

RS functional MR BOLD data were acquired from the 1000 Functional Connectomes Project, which is a publicly accessible database that is available for download and retrospective analysis (*www.nitrc.org/projects/fcon_1000*) (23). Specifically, data from 30 (15 women, 15 men; mean age, 21.3 years; age range, 18–25 years) of 198 subjects recruited as part of larger studies conducted in Beijing, China, were processed and analyzed. All right-handed undergraduate or graduate students at Beijing Normal University were eligible for MR imaging. Exclusion criteria included a history of head injury, psychiatric disorder, neurologic disorder, or alcohol and/or substance abuse (24–26); however, no subjects were excluded on the basis of these criteria. At least 15 subjects from the total pool were excluded because of excessive head movement during imaging (26). All subjects provided written informed consent, and this study was approved by the institutional review board of the State Key Laboratory of Cognitive Neuroscience and Learning, Beijing Normal University (24–26).

MR Imaging

The 30 subjects were examined with a 3.0-T MR imaging unit (Trio; Siemens, Erlangen, Germany) to collect T1-weighted structural anatomic (magnetization-prepared rapid acquisition gradient echo) MR and RS functional MR BOLD data. RS functional MR imaging was performed by using echo-planar imaging (repetition time msec/echo time msec, 2000/30; field of view, 200 × 200 mm; matrix, 64 × 64; 33 axial sections; 3-mm section thickness; 0.6-mm section gap; voxel resolution, 3.125 × 3.125 × 3.6 mm). The subjects did not perform a task, but they were asked to keep their eyes closed for the 7.5-minute RS functional MR examination (24,25).

Data Processing

All data were motion corrected and normalized to a standard template by using statistical parametric mapping software (SPM8; *www.fil.ion.ucl.ac.uk/spm/software/spm8*) (27). The structural T1-weighted images were segmented into gray matter and cerebrospinal fluid by using the statistical parametric mapping new segment tool. Segmentation maps were resampled to the space of the normalized functional MR imaging data for use as masks in postprocessing. To investigate changes in network metrics over a range of BOLD signal acquisition durations, each subject's motion-corrected normalized 7.5-minute RS functional MR imaging run was truncated into 30-second bins, with BOLD signal acquisition durations ranging from 1.5 to 7.5 minutes, thereby generating 13 individual RS functional MR imaging data sets. Preprocessing of time-binned data included regression of motion parameters, nuisance signals (white matter and ventricular mean signal from the segmentation maps), and global signal, followed by band-pass filtering at 0.01–0.1 Hz to isolate the low-frequency fluctuations characteristic of RS connectivity. Data were then parcellated into 116 regions by using the Automated Anatomical Labeling atlas (28), as implemented with WFU-PickAtlas software (*www.ansir.wfubmc.edu*) (29), and masked with the gray matter segmentation map to limit the nodes to gray matter structures. This resulted in an averaged functional MR imaging time series of 116 regions (nodes) for each subject, which was used for subsequent graph theory connectivity analysis.

Functional Network Connectivity and Graph Theoretical Analyses

To establish the presence of functional connectivity between the parcellated regions (nodes), the Pearson correlation was computed between all pairs of node time series to generate a 116 × 116 Cij for each time bin and subject. The Cij was thresholded and dichotomized to generate a binarized adjacency matrix for each subject and acquisition duration at a range of network costs (0.1–0.5) (Appendix E1 [online]), with removal of any isolated nodes. Network cost is defined as the ratio of the number of edges (connections) in a network to the maximum possible number of edges (6,30). Graph theory metrics (small worldness, local efficiency, and global efficiency) were then computed from the adjacency matrix by using Matlab 2010a software (MathWorks, Natick, Mass), including the Matlab Boost Graphics Library, as well as the Brain Connectivity Toolbox (*www.brain-connectivity-toolbox.net*) (31) in the standard fashion (18) to evaluate whole-brain functional connectivity for each time-binned RS functional MR imaging data set at each cost for every subject (Appendix E1 [online]). These particular graph metrics were chosen because they have been used to study a variety of clinically important neurodegenerative and psychiatric disorders affecting the central nervous system (10–17). Computations were implemented on a 15-node 30-core computer cluster

to enable analysis of the massive number of resulting brain networks (approximately 2000) in a computationally tractable time frame.

Statistical Analyses

Two-way analysis of variance (ANOVA) was conducted to explore the affect of RS functional MR imaging duration on the magnitude of computed network metrics at different costs. BOLD signal acquisition duration (1.5–7.5 minutes in bins incrementally larger by 30 seconds) and cost (0.1, 0.2, 0.3, 0.4, and 0.5) were used as independent variables. Graph theory network metrics (small worldness, local efficiency, global efficiency) and correlation coefficient threshold were used as dependent variables. To determine the stability of correlations across durations, one-way ANOVA was conducted by using Cij-associated standard deviations (SD), with BOLD signal acquisition duration (1.5–7.5 minutes in bins incrementally larger by 30 seconds) as the independent variable and SD as the dependent variable. The SD associated with correlations of all nodal RS functional MR time series provides a global measure of stability of the correlation values, as opposed to mean correlation values, which would merely approach zero. The Cij-associated SD was generated as follows: SD was first computed for each subject's Cij (across all elements of the Cij) at each BOLD signal acquisition duration (time bin). This generated 13 SDs (one per time bin) for each of the 30 subjects, which were used for statistical analysis. SD was then averaged across subjects at each time bin, reducing the data to 1 SD per time bin (13 time bins) for graphing. This enabled assessment of the changes in correlation coefficient variability (SD) as a function of increasing BOLD signal data collection duration.

Posthoc analyses with the Dunnett test were conducted to further explore significant effects revealed by ANOVA by using the longest BOLD signal acquisition duration (7.5 minutes) as the control group for pairwise comparisons. All statistical analyses were performed with statistical software (SPSS, version 16.0; SPSS, Chicago, Ill).

Results

Small worldness, local efficiency, and global efficiency were computed for every subject at each BOLD signal data collection duration and cost (Table 1, Fig 1). Plots of these data have a nearly horizontal line, with little difference between the magnitude of computed graph metrics at each data collection duration. This suggests almost immediate graph theory metric data stability. Two-way ANOVA revealed no significant interaction of BOLD signal acquisition duration by cost for small worldness ($F[12, 1885] = 0.527$, $P > .05$), local efficiency ($F[12, 1885] = 0.1.329$, $P > .05$), or global efficiency ($F[12, 1885] = 1.372$, $P > .05$). There was no significant main effect of BOLD signal acquisition duration on the magnitude of the small-world metric at any cost ($F[12, 1885] = 1.716$, $P > .05$). This indicated that small-world values computed by using the 1.5-minute BOLD signal acquisition duration are no different than those computed by using the 7.5-minute BOLD data acquisition duration (Fig 1a). ANOVA, however, revealed a significant but relatively small effect of BOLD signal acquisition duration on the magnitude of local efficiency ($F[12, 1885] = 3.639$, $P < .001$, partial $\eta^2 = 0.023$] and global efficiency ($F[12, 1885] = 3.488$, $P < .001$, partial $\eta^2 = 0.022$].

For local efficiency, Dunnett post hoc analyses revealed significant differences associated with BOLD signal data collection duration at costs of 0.1 and 0.2 only, as follows: At a cost of 0.1, there was a significant 6.8% difference (95% confidence interval [CI]: −0.0672, −0.0078; $P = .005$) between the magnitude of local efficiency computed by using 7.5 and 2.0 minutes of BOLD data (Fig 1b). At a cost of 0.2, there was a significant 3.1% difference (95% CI: −0.0419, −0.0001; $P = .048$) between the magnitude of local efficiency computed by using 7.5 and 3 minutes of BOLD data (Fig 1b).

For global efficiency, Dunnett post hoc analyses revealed significant differences associated with BOLD signal data collection duration at costs of 0.4 and 0.5 only, as follows: At a cost of 0.4, there was a significant 1.3% difference (95% CI: −0.0134, −0.0011; $P = .011$) between the magnitude of global efficiency computed by using 7.5 and 1.5 minutes of BOLD data (Fig 1c). At a cost of 0.5, there was a significant 1.1% difference (95% CI: −0.0117, −0.0021; $P = .001$) between the magnitude of global efficiency computed by using 7.5 and 1.5 minutes of BOLD data (Fig 1c).

We evaluated the effect of RS functional MR imaging BOLD signal acquisition duration on correlation coefficient stability associated with functional connectivity matrices (correlation coefficient SD and correlation threshold) (Table 2, Fig 2). Plots of these data show that variability (SD) in the Cij and magnitude of the correlation threshold decrease with increasing BOLD signal acquisition duration but that there is little change in magnitude after approximately 5 minutes of data collection.

One-way ANOVA revealed a significant effect of BOLD signal acquisition duration on Cij-related SD ($F[12, 389] = 104.078$, $P < .001$). Dunnett post hoc analyses revealed significant differences ($P < .01$) between correlation SD values calculated by using 7.5-minute data and short acquisition durations ranging from 1.5 to 4.5 minutes (Fig 2a, Table 3).

Two-way ANOVA revealed a significant disordinal interaction of signal acquisition duration by cost for the correlation threshold, such that decreases in correlation threshold magnitude associated with longer acquisition durations were greater with increasing cost ($F[48, 1885] = 2.228$, $P < .001$). The effect size associated with this interaction, however, was quite small (partial $\eta^2 = 0.054$). ANOVA also revealed a main effect of BOLD signal acquisition duration on correlation threshold magnitude ($F[12, 1885] = 458.695$, $P < .001$, partial $\eta^2 = 0.745$). Dunnett post hoc analyses revealed significant differences between correlation thresholds calculated by using different BOLD signal data collection durations at all costs, as follows: At a cost of 0.1, there were significant differences ($P < .017$) between correlation threshold values calculated by using the 7.5-minute data and acquisition durations of 1.5–4.0 minutes (Fig 2b, Table 3). At

Table 1

Effect of BOLD Signal Acquisition Duration on Stability of Graph Theory Network Metrics

Cost	1.5-minute BOLD Signal Acquisition	2.0-minute BOLD Signal Acquisition	2.5-minute BOLD Signal Acquisition	3.0-minute BOLD Signal Acquisition	3.5-minute BOLD Signal Acquisition	4.0-minute BOLD Signal Acquisition	4.5-minute BOLD Signal Acquisition	5.0-minute BOLD Signal Acquisition	5.5-minute BOLD Signal Acquisition	6.0-minute BOLD Signal Acquisition	6.5-minute BOLD Signal Acquisition	7.0-minute BOLD Signal Acquisition	7.5-minute BOLD Signal Acquisition
Small Worldness													
0.1	3.59 ± 0.97	3.51 ± 0.74	3.47 ± 0.69	3.62 ± 0.84	3.51 ± 0.88	3.64 ± 0.87	3.82 ± 0.88	3.69 ± 0.79	3.65 ± 0.68	3.75 ± 0.78	3.76 ± 0.82	3.82 ± 0.82	3.66 ± 0.80
0.2	2.78 ± 0.41	2.76 ± 0.31	2.71 ± 0.28	2.79 ± 0.38	2.73 ± 0.31	2.78 ± 0.30	2.89 ± 0.26	2.88 ± 0.28	2.88 ± 0.26	2.91 ± 0.31	2.91 ± 0.31	2.90 ± 0.28	2.90 ± 0.33
0.3	2.31 ± 0.20	2.30 ± 0.14	2.27 ± 0.13	2.28 ± 0.15	2.27 ± 0.15	2.29 ± 0.14	2.33 ± 0.15	2.33 ± 0.15	2.34 ± 0.16	2.35 ± 0.16	2.36 ± 0.16	2.36 ± 0.16	2.36 ± 0.18
0.4	2.03 ± 0.12	2.02 ± 0.09	2.00 ± 0.08	2.01 ± 0.08	2.00 ± 0.09	2.00 ± 0.09	2.00 ± 0.10	2.00 ± 0.10	2.00 ± 0.10	2.01 ± 0.10	2.03 ± 0.10	2.03 ± 0.11	2.01 ± 0.12
0.5	1.85 ± 0.09	1.83 ± 0.07	1.83 ± 0.07	1.82 ± 0.07	1.82 ± 0.07	1.80 ± 0.07	1.80 ± 0.07	1.80 ± 0.08	1.80 ± 0.08	1.80 ± 0.08	1.81 ± 0.08	1.82 ± 0.09	1.81 ± 0.09
Local Efficiency													
0.1	0.53 ± 0.04	0.52 ± 0.03	0.53 ± 0.05	0.53 ± 0.04	0.53 ± 0.04	0.53 ± 0.04	0.53 ± 0.04	0.54 ± 0.04	0.54 ± 0.05	0.54 ± 0.05	0.55 ± 0.04	0.55 ± 0.04	0.56 ± 0.04
0.2	0.66 ± 0.03	0.66 ± 0.02	0.65 ± 0.03	0.65 ± 0.03	0.65 ± 0.03	0.65 ± 0.03	0.65 ± 0.03	0.65 ± 0.03	0.66 ± 0.03	0.66 ± 0.03	0.67 ± 0.03	0.66 ± 0.03	0.67 ± 0.03
0.3	0.72 ± 0.02	0.71 ± 0.01	0.71 ± 0.02	0.70 ± 0.02	0.71 ± 0.02	0.70 ± 0.02	0.71 ± 0.02	0.70 ± 0.02	0.71 ± 0.02	0.71 ± 0.02	0.72 ± 0.02	0.71 ± 0.02	0.72 ± 0.02
0.4	0.75 ± 0.01	0.74 ± 0.01	0.74 ± 0.02	0.74 ± 0.02	0.74 ± 0.02	0.74 ± 0.02	0.73 ± 0.02	0.73 ± 0.02	0.74 ± 0.02	0.74 ± 0.02	0.74 ± 0.02	0.74 ± 0.02	0.74 ± 0.02
0.5	0.76 ± 0.01	076 ± 0.01	0.76 ± 0.01	0.75 ± 0.01	0.76 ± 0.01	0.75 ± 0.02	0.75 ± 0.02	0.75 ± 0.02	0.75 ± 0.02	0.75 ± 0.02	0.75 ± 0.02	0.75 ± 0.02	0.76 ± 0.02
Global Efficiency													
0.1	0.30 ± 0.02	0.30 ± 0.02	0.30 ± 0.03	0.30 ± 0.03	0.30 ± 0.02	0.30 ± 0.02	0.30 ± 0.02	0.30 ± 0.02	0.30 ± 0.03	0.30 ± 0.03	0.29 ± 0.03	0.29 ± 0.03	0.29 ± 0.03
0.2	0.43 ± 0.01	0.43 ± 0.01	0.43 ± 0.02	0.43 ± 0.02	0.43 ± 0.02	0.43 ± 0.02	0.43 ± 0.01	0.44 ± 0.01	0.43 ± 0.01	0.43 ± 0.02	0.43 ± 0.02	0.43 ± 0.01	0.43 ± 0.01
0.3	0.50 ± 0.01	0.50 ± 0.01	0.51 ± 0.01	0.51 ± 0.01	0.51 ± 0.01	0.51 ± 0.01	0.51 ± 0.01	0.51 ± 0.01	0.51 ± 0.01	0.51 ± 0.01	0.51 ± 0.01	0.51 ± 0.01	0.51 ± 0.01
0.4	0.56 ± 0.01	0.56 ± 0.01	0.56 ± 0.01	0.56 ± 0.01	0.56 ± 0.01	0.56 ± 0.01	0.57 ± 0.01	0.57 ± 0.01	0.57 ± 0.01	0.56 ± 0.01	0.56 ± 0.01	0.56 ± 0.01	0.56 ± 0.01
0.5	0.60 ± 0.01	0.60 ± 0.01	0.61 ± 0.01	0.61 ± 0.01	0.61 ± 0.01	0.61 ± 0.01	0.61 ± 0.01	0.61 ± 0.01	0.61 ± 0.01	0.61 ± 0.01	0.61 ± 0.01	0.61 ± 0.01	0.61 ± 0.01

Note.—Data are means ± SDs.

costs of 0.2–0.5, there were significant differences ($P < .019$) between correlation threshold values calculated by using the 7.5-minute data and acquisition durations of 1.5–4.5 minutes (Fig 2b, Table 3). Taken together, these data suggest that correlation data (correlation coefficient SD and correlation threshold) stabilize after 4.5–5 minutes of BOLD signal data collection.

Discussion

In order for functional network connectivity methods to be useful clinically, efficient and cost-effective MR imaging protocols must be established that provide sufficient data for analysis by using the shortest reasonable data acquisition duration, which—to our knowledge—has not been established for graph theoretical analyses. In the present study, we have shown that specific frequently used graph theory metrics of brain network connectivity (small worldness, local efficiency, and global efficiency) may be accurately computed from as little as 1.5–2.0 minutes of RS functional MR imaging BOLD signal. This relatively short 1.5–2.0-minute BOLD data collection duration for graph metric stabilization is contrasted with the relatively longer 5-minute data acquisition duration required for stabilization of the correlation coefficient output. In particular, these data are consistent with our hypothesis that the correlation coefficient data from the Cij and the corresponding computed graph theory metrics stabilize along different temporal trajectories, and they suggest that different RS functional MR imaging BOLD signal acquisition durations may be used depending on the outcome of interest. Although these data were consistent with our proposed hypothesis, the magnitude of difference in BOLD collection duration required for data stability between the correlation and graph theory output was somewhat unexpected. One possible explanation for the relatively rapid stabilization of the graph theory data are that the intrinsic relationships between ROIs that underlie the graph theory output are present within the Cij at the earliest time points, despite

Figure 1

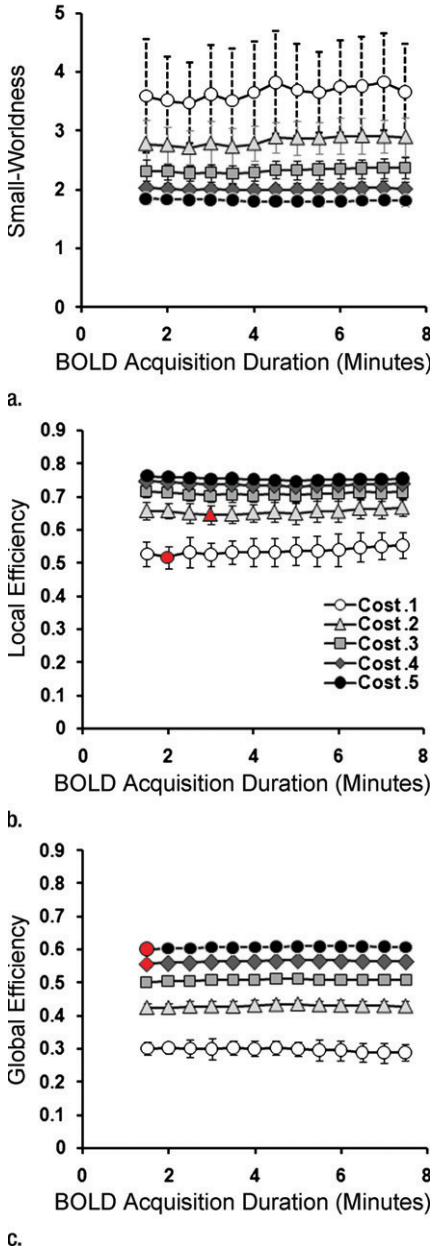

Figure 1: Graphs show magnitude (mean ± SD) of **(a)** small worldness, **(b)** local efficiency, and **(c)** global efficiency plotted by duration of BOLD signal acquisition (1.5–7.5 minutes in 30-sec bins) for each cost (0.1, 0.2, 0.3, 0.4, 0.5). Red-filled shapes indicate significant differences in the magnitude of a graph metric associated with a given BOLD signal acquisition duration compared with the magnitude of the same graph metric when computed by using 7.5 minutes of BOLD data. These data form nearly horizontal lines, with little difference between the magnitude of the computed graph metrics at each data collection duration. Specifically, at higher costs (0.3–0.5), there is rapid stabilization in the magnitude of small worldness and local efficiency by 1.5 minutes and stabilization in the magnitude of global efficiency by 2.0 minutes.

the relatively high magnitude of correlation coefficient variability. The signal used to calculate graph metrics may be much higher than the noise (variability) within the Cij across all data collection durations. Our preliminary analyses of bin-to-bin differences in network architecture suggest up to an 80% commonality in edges at a particular cost, even between the earliest time bins. The connectome data sets (*www.nitrc.org/projects/fcon_1000*) can provide a rich resource for further investigation of the temporal dynamics underlying network stabilization.

In the present study, we evaluated changes in correlation threshold associated with increasing BOLD signal acquisition duration as another method with which to evaluate differences between the temporal trajectory of correlation stabilization. Similar to the Cij-related SD stabilization results, these data suggest that correlation threshold also stabilizes at 4.5–5 minutes. It is possible that the magnitude of variability within the correlation coefficient data may drive the changes in the cost-related threshold. As such, when variability in the Cij is high, a correlation coefficient of greater magnitude is required to maintain a constant number of edges for each cost.

In this study, we used specific network costs to identify appropriate correlation thresholds. Such application of cost is useful, as it facilitates comparison of data across individual subjects by generating comparable networks of equivalent size. Costs from 0.1 to 0.5 span the range of meaningful networks for RS functional MR imaging data and were chosen for this investigation on the basis of costs commonly described in the literature (3,4,30,32,33). In the present study, local and global efficiency increased and small worldness decreased as cost increased. The magnitude of local efficiency, global efficiency, and small worldness at each cost were similar to values reported for healthy subjects in prior studies in which these graph theory metrics were used (3,4,30,32,33). Interestingly, the difference between global efficiency and cost reached a maximum at a cost of 0.2, as reported by Achard and Bullmore (3), who used a wavelet-based approach to graph theory analysis. As such, a cost of 0.2 or 0.3 may be an appropriate choice to apply in future clinical investigations in which graph theoretical analyses are used. Additional studies, however, may be necessary to determine the optimal cost with which to investigate abnormal brain networks.

The present data enabled us to confirm previous findings reported by Van Dijk and colleagues (22); this suggests a minimum BOLD data collection duration of approximately 5–6 minutes for stabilization of average correlation strengths, even though the techniques used to evaluate the correlation data in the Van Dijk et al study were different from the techniques used in our study. In the Van Dijk study, stability between default, attention, and reference networks was evaluated by using RS functional MR imaging BOLD data collected between 2 and 12 minutes. Correlation strengths within and between default, attention, and reference networks were shown to stabilize after acquisition of approximately 5 minutes of BOLD data (22). Noise in the correlation data defined as spurious correlations also decreased in approximate proportion to the square root of the sampling time, reaching stable levels after approximately 5–6 minutes of BOLD signal acquisition (22). Rather than evaluate correlation strengths between specific subnetworks and changes in spurious correlations as did Van Dijk and colleagues, we evaluated variability within the overall correlation matrices by identifying changes in SD across acquisition durations, which also stabilized after acquisition of 5 minutes of BOLD signal.

This study had limitations. RS functional MR imaging data used in this study were collected with a 3.0-T MR imaging

Table 2

Effect of BOLD Signal Acquisition Duration on Measures of Correlation Coefficient Stability

Cost	1.5-minute BOLD Signal Acquisition	2.0-minute BOLD Signal Acquisition	2.5-minute BOLD Signal Acquisition	3.0-minute BOLD Signal Acquisition	3.5-minute BOLD Signal Acquisition	4.0-minute BOLD Signal Acquisition	4.5-minute BOLD Signal Acquisition	5.0-minute BOLD Signal Acquisition	5.5-minute BOLD Signal Acquisition	6.0-minute BOLD Signal Acquisition	6.5-minute BOLD Signal Acquisition	7.0-minute BOLD Signal Acquisition	7.5-minute BOLD Signal Acquisition
	Correlation Coefficient SD												
NA	0.35 ± 0.02	0.32 ± 0.02	0.30 ± 0.02	0.29 ± 0.02	0.28 ± 0.02	0.27 ± 0.02	0.26 ± 0.02	0.25 ± 0.02	0.25 ± 0.02	0.25 ± 0.02	0.25 ± 0.02	0.25 ± 0.02	0.25 ± 0.02
	Correlation Coefficient Threshold												
0.1	0.59 ± 0.03	0.55 ± 0.03	0.52 ± 0.03	0.49 ± 0.03	0.48 ± 0.03	0.47 ± 0.04	0.46 ± 0.03	0.45 ± 0.03	0.45 ± 0.03	0.44 ± 0.03	0.44 ± 0.04	0.44 ± 0.03	0.44 ± 0.04
0.2	0.48 ± 0.02	0.44 ± 0.02	0.41 ± 0.03	0.39 ± 0.02	0.37 ± 0.03	0.36 ± 0.03	0.35 ± 0.03	0.34 ± 0.03	0.34 ± 0.03	0.33 ± 0.03	0.33 ± 0.03	0.33 ± 0.03	0.33 ± 0.03
0.3	0.40 ± 0.02	0.36 ± 0.02	0.33 ± 0.02	0.31 ± 0.02	0.30 ± 0.02	0.29 ± 0.03	0.28 ± 0.02	0.27 ± 0.02	0.26 ± 0.02	0.26 ± 0.02	0.26 ± 0.02	0.26 ± 0.02	0.25 ± 0.02
0.4	0.33 ± 0.02	0.29 ± 0.02	0.27 ± 0.02	0.25 ± 0.02	0.24 ± 0.02	0.23 ± 0.02	0.22 ± 0.02	0.21 ± 0.02	0.21 ± 0.02	0.21 ± 0.02	0.20 ± 0.02	0.20 ± 0.02	0.20 ± 0.02
0.5	0.26 ± 0.02	0.23 ± 0.02	0.22 ± 0.02	0.20 ± 0.02	0.19 ± 0.02	0.18 ± 0.02	0.18 ± 0.02	0.17 ± 0.01	0.16 ± 0.01	0.16 ± 0.02	0.16 ± 0.01	0.16 ± 0.02	0.16 ± 0.02

Note.—Data are means ± SDs. NA = not applicable.

Table 3

Dunnett Post Hoc Analysis Data for Measures of Correlation Coefficient Stability Associated with BOLD Signal Acquisition Duration

Cost	1.5-minute BOLD Signal Acquisition	2.0-minute BOLD Signal Acquisition	2.5-minute BOLD Signal Acquisition	3.0-minute BOLD Signal Acquisition	3.5-minute BOLD Signal Acquisition	4.0-minute BOLD Signal Acquisition	4.5-minute BOLD Signal Acquisition	5.0-minute BOLD Signal Acquisition	5.5-minute BOLD Signal Acquisition	6.0-minute BOLD Signal Acquisition	6.5-minute BOLD Signal Acquisition	7.0-minute BOLD Signal Acquisition
	Correlation Coefficient SD											
NA	<.001 (0.0946, 0.1206)	<.001 (0.0632, 0.0892)	<.001 (0.0456, 0.0716)	<.001 (0.0283, 0.0543)	<.001 (0.0208, 0.0468)	<.001 (0.0103, 0.0363)	.009 (0.0026, 0.0286)	.504	.759	.996	>.99	>.99
	Correlation Coefficient Threshold											
0.1	<.001 (0.1279, 0.1752)	<.001 (0.0845, 0.1318)	<.001 (0.0553, 0.1027)	<.001 (0.0291, 0.0764)	<.001 (0.0184, 0.0657)	<.016 (0.0034, 0.0507)	.304	.997	.999	>.99	>.99	>.99
0.2	<.001 (0.1347, 0.1735)	<.001 (0.0914, 0.1302)	<.001 (0.0650, 0.1038)	<.001 (0.0401, 0.0789)	<.001 (0.0267, 0.0664)	<.001 (0.0136, 0.0524)	<.018 (0.0025, 0.0413)	.638	.649	.991	.999	>.99
0.3	<.001 (0.1265, 0.1594)	<.001 (0.0858, 0.1186)	<.001 (0.0640, 0.0969)	<.001 (0.0409, 0.0738)	<.001 (0.0311, 0.0639)	<.001 (0.0170, 0.0498)	<.001 (0.0076, 0.0404)	.233	.397	.934	.991	>.99
0.4	<.001 (0.1115, 0.1392)	<.001 (0.0784, 0.1061)	<.001 (0.0575, 0.0853)	<.001 (0.0373, 0.0651)	<.001 (0.0288, 0.0566)	<.001 (0.0165, 0.0443)	<.001 (0.0081, 0.0359)	.105	.266	.786	.979	>.99
0.5	<.001 (0.0948, 0.1182)	<.001 (0.0658, 0.0891)	<.001 (0.0486, 0.0720)	<.001 (0.0315, 0.0548)	<.001 (0.0245, 0.0479)	<.001 (0.0139, 0.0373)	<.001 (0.0082, 0.0316)	.08	.338	.776	.992	>.99

Note.—Dunnett posthoc analysis data using the longest BOLD signal acquisition duration (7.5 min) as the control group for pairwise comparisons. Data are *P* values, and data in parentheses are 95% CIs. NA = not applicable.

Figure 2

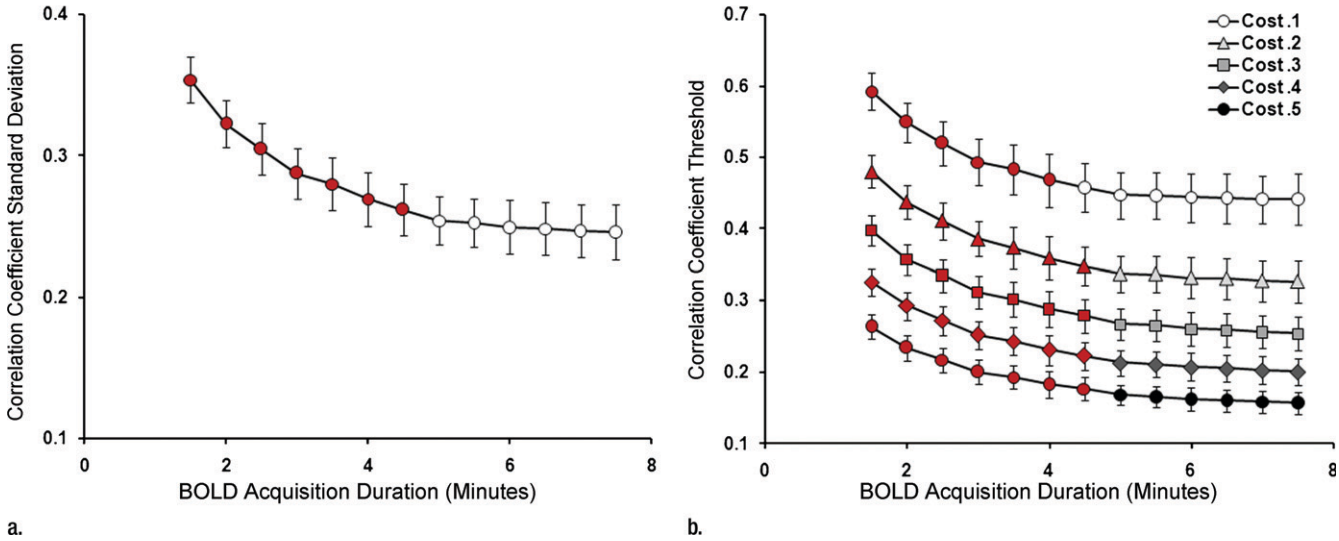

Figure 2: Magnitude (mean ± SD) of **(a)** computed Cij and SD and **(b)** correlation coefficient threshold, plotted by duration of BOLD signal acquisition (1.5–7.5 minutes in 30-sec bins) and for correlation threshold at each cost (0.1, 0.2, 0.3, 0.4, 0.5). Red-filled shapes indicate a significant difference in the magnitude of the computed value associated with a given BOLD signal acquisition duration compared with the magnitude when computed by using 7.5 minutes of BOLD data (Table 3). Magnitude of correlation data output decreases as BOLD signal acquisition duration increases, with little change in magnitude after approximately 5 minutes of data collection. Specifically, there is stabilization in the magnitude of Cij-associated SD by 5 minutes and stabilization of correlation threshold by 4.5–5 minutes, depending on cost. The 4.5–5.0-minute BOLD data collection duration required for correlation data stabilization is contrasted with the relatively short 1.5–2.0-minute data acquisition duration required for stabilization of the graph theory metrics (Fig 1).

unit. As such, these results may not be generalizable to RS functional MR imaging BOLD signal collected at other field strengths. Only a small selection of possible graph metrics were tested; thus, it is unknown if short BOLD signal acquisition durations are sufficient for all graph metrics. The subjects in this study were healthy volunteers, without neurologic or psychiatric abnormalities. Thus, the present data have not been validated in clinical populations, where abnormalities of the central nervous system may alter the stability of graph metrics, possibly requiring longer BOLD data collection durations. Test-retest reliability for relatively short-duration collections of RS functional MR imaging BOLD data, such as those described by Shehzad and colleagues (34) with longer 6–7 minute collection durations, have not been conducted to determine if these data are similarly consistent within subjects across time. Although our data suggest that graph theory metrics may stabilize after relatively short 1.5–2.0-minute BOLD data acquisition durations, the shortest possible data collection duration for graph theory metric stability remains unknown.

In conclusion, as little as 2 minutes of RS functional MR imaging BOLD signal may be sufficient to enable one to accurately calculate frequently used graph theory metrics of brain network connectivity. This finding suggests that the addition of these methods to clinical imaging protocols may be feasible and cost-effective, even in populations that pose challenges to routine imaging, such as young children and critically ill patients.

Acknowledgments: We thank Benjamin Wagner of the Advanced NeuroScience Imaging Research (ANSIR) Laboratory in the Department of Radiology at Wake Forest University School of Medicine for his expert computer programming assistance. We also thank the Foundation of the American Society of Neuroradiology for their generous support of this work via the Fellowship in Basic Science Research. We are also grateful to the scientists of the State Key Laboratory of Cognitive Neuroscience and Learning, Beijing Normal University, for generously providing the RS functional MR imaging BOLD data via the 1000 Functional Connectomes Project.

Disclosures of Potential Conflicts of Interest: C.T.W. Financial activities related to the present article: none to disclose. Financial activities not related to the present article: none to disclose. Other relationships: none to disclose. **R.C.** Financial activities related to the present article: none to disclose. Financial activities not related to the present article: none to disclose. Other relationships: none to disclose. **J.A.M.** No potential conflicts of interest to disclose.

References

1. Watts DJ, Strogatz SH. Collective dynamics of 'small-world' networks. Nature 1998; 393(6684):440–442.
2. Bassett DS, Bullmore ET. Human brain networks in health and disease. Curr Opin Neurol 2009;22(4):340–347.
3. Achard S, Bullmore E. Efficiency and cost of economical brain functional networks. PLOS Comput Biol 2007;3(2):e17.
4. Bassett DS, Bullmore E. Small-world brain networks. Neuroscientist 2006;12(6):512–523.
5. Lago-Fernández LF, Huerta R, Corbacho F, Sigüenza JA. Fast response and temporal coherent oscillations in small-world networks. Phys Rev Lett 2000;84(12):2758–2761.

6. Latora V, Marchiori M. Efficient behavior of small-world networks. Phys Rev Lett 2001; 87(19):198701.
7. Masuda N, Aihara K. Global and local synchrony of coupled neurons in small-world networks. Biol Cybern 2004;90(4):302–309.
8. Sporns O, Zwi JD. The small world of the cerebral cortex. Neuroinformatics 2004;2(2): 145–162.
9. Buzsaki G. Rhythms of the brain. New York, NY: Oxford University Press, 2006; 464.
10. Bokde AL, Ewers M, Hampel H. Assessing neuronal networks: understanding Alzheimer's disease. Prog Neurobiol 2009;89(2): 125–133.
11. Dickerson BC, Sperling RA. Large-scale functional brain network abnormalities in Alzheimer's disease: insights from functional neuroimaging. Behav Neurol 2009;21(1): 63–75.
12. Guye M, Bettus G, Bartolomei F, Cozzone PJ. Graph theoretical analysis of structural and functional connectivity MRI in normal and pathological brain networks. MAGMA 2010;23(5-6):409–421.
13. He Y, Chen Z, Gong G, Evans A. Neuronal networks in Alzheimer's disease. Neuroscientist 2009;15(4):333–350.
14. He Y, Dagher A, Chen Z, et al. Impaired small-world efficiency in structural cortical networks in multiple sclerosis associated with white matter lesion load. Brain 2009; 132(Pt 12):3366–3379.
15. Supekar K, Menon V, Rubin D, Musen M, Greicius MD. Network analysis of intrinsic functional brain connectivity in Alzheimer's disease. PLOS Comput Biol 2008;4(6): e1000100.
16. Wang L, Zhu C, He Y, et al. Altered small-world brain functional networks in children with attention-deficit/hyperactivity disorder. Hum Brain Mapp 2009;30(2):638–649.
17. Zhang HY, Wang SJ, Liu B, et al. Resting brain connectivity: changes during the progress of Alzheimer disease. Radiology 2010; 256(2):598–606.
18. Bullmore E, Sporns O. Complex brain networks: graph theoretical analysis of structural and functional systems. Nat Rev Neurosci 2009;10(3):186–198.
19. Wang J, Zuo X, He Y. Graph-based network analysis of resting-state functional MRI. Front Syst Neurosci 2010;4:16.
20. Salvador R, Suckling J, Coleman MR, Pickard JD, Menon D, Bullmore E. Neurophysiological architecture of functional magnetic resonance images of human brain. Cereb Cortex 2005;15(9):1332–1342.
21. Achard S, Salvador R, Whitcher B, Suckling J, Bullmore E. A resilient, low-frequency, small-world human brain functional network with highly connected association cortical hubs. J Neurosci 2006;26(1):63–72.
22. Van Dijk KR, Hedden T, Venkataraman A, Evans KC, Lazar SW, Buckner RL. Intrinsic functional connectivity as a tool for human connectomics: theory, properties, and optimization. J Neurophysiol 2010;103(1):297–321.
23. Biswal BB, Mennes M, Zuo XN, et al. Toward discovery science of human brain function. Proc Natl Acad Sci U S A 2010;107(10): 4734–4739.
24. Liu D, Yan C, Ren J, Yao L, Kiviniemi VJ, Zang Y. Using coherence to measure regional homogeneity of resting-state FMRI signal. Front Syst Neurosci 2010;4:24.
25. Yan H, Zuo XN, Wang DY, et al. Hemispheric asymmetry in cognitive division of anterior cingulate cortex: a resting-state functional connectivity study. Neuroimage 2009;47(4):1579–1589.
26. Tian L, Wang J, Yan C, He Y. Hemisphere- and gender-related differences in small-world brain networks: a resting-state functional MRI study. Neuroimage 2010;54(1): 191–202.
27. Friston KJ, Holmes AP, Worsley KJ, Poline JP, Frith CD, Frackowiak RS. Statistical parametric maps in functional imaging: a general linear approach. Hum Brain Mapp 1994;2(4):189–210.
28. Tzourio-Mazoyer N, Landeau B, Papathanassiou D, et al. Automated anatomical labeling of activations in SPM using a macroscopic anatomical parcellation of the MNI MRI single-subject brain. Neuroimage 2002; 15(1):273–289.
29. Maldjian JA, Laurienti PJ, Kraft RA, Burdette JH. An automated method for neuroanatomic and cytoarchitectonic atlas-based interrogation of fMRI data sets. Neuroimage 2003;19(3):1233–1239.
30. Latora V, Marchiori M. Economic small-world behavior in weighted networks. Eur Phys J B Condens Matter Complex Syst 2003;32(2):249–263.
31. Rubinov M, Sporns O. Complex network measures of brain connectivity: uses and interpretations. Neuroimage 2010;52(3): 1059–1069.
32. Fan Y, Shi F, Smith JK, Lin W, Gilmore JH, Shen D. Brain anatomical networks in early human brain development. Neuroimage 2010; 54(3):1862–1871.
33. Fornito A, Zalesky A, Bullmore ET. Network scaling effects in graph analytic studies of human resting-state FMRI data. Front Syst Neurosci 2010;4:22.
34. Shehzad Z, Kelly AM, Reiss PT, et al. The resting brain: unconstrained yet reliable. Cereb Cortex 2009;19(10):2209–2229.
35. Milo R, Shen-Orr S, Itzkovitz S, Kashtan N, Chklovskii D, Alon U. Network motifs: simple building blocks of complex networks. Science 2002;298(5594):824–827.
36. Humphries MD, Gurney K, Prescott TJ. The brainstem reticular formation is a small-world, not scale-free, network. Proc Biol Sci 2006;273(1585):503–511.